LA-UR-01-4788
Approved for public release; distribution is unlimited.

Title: **Study of Threshold Reaction Rates Inside and on the Surface of a 0.8-GeV Proton-Irradiated Thick W-Na Target**

Author(s): Yury E. Titarenko, Vyacheslav F. Batyaev, Evgeny I. Karpikhin, Valery M. Zhivun, Alexsander B. Koldobsky, Ruslan D. Mulambetov, Dmitry V. Fischenko, Svetlana V. Kvasova, Andry M. Voloschenko, Stepan G. Mashnik, Richard E. Prael, Hideshi Yasuda

Submitted to:

http://lib-www.lanl.gov/la-pubs/00818512.pdf

STUDY OF THRESHOLD REACTION RATES INSIDE AND ON THE SURFACE OF A 0.8-GEV PROTON-IRRADIATED THICK W-NA TARGET

Yury E. Titarenko, Vyacheslav F. Batyaev, Evgeny I. Karpikhin,
Valery M. Zhivun, Aleksander B. Koldobsky, Ruslan D. Mulambetov,
Dmitry V. Fishchenko, Svetlana V. Kvasova
Institute for Theoretical and Experimental Physics,
B. Cheremushkinskaya 25, Moscow, 117259, Russia
Andrey M. Voloschenko
Keldysh Institute of Applied Mathematics, Miusskaya Sq. 4, 125047 Moscow, Russia
Stepan G. Mashnik, Richard E. Prael
Los Alamos National Laboratory, Los Alamos, NM 87545, USA
Hideshi Yasuda
Japan Atomic Energy Research Institute, Tokai, Ibaraki, 319-1195, Japan

August 10, 2001

ABSTRACT

The preliminary results are presented of the experimental determination of threshold reaction rates in experimental samples made of Al, Co, Bi, In, Au et al. placed both inside and on the surface of extended thick W-Na target irradiated with 0.8 GeV protons. The target consists of 25 alternating discs each 150 mm in diameter: 5 tungsten discs are 20 mm thick, 7 tungsten discs are 40 mm thick, and 13 sodium discs are 40 mm thick. The relative position of discs is matched with the aim of flattening the neutron field along the target surface. The comparison is made of the measured rates with results of their simulation using LAHET and KASKAD-S codes, and MENDL2, MENDL2P, SADKO-2, and ABBN-93 databases. The results are of interest both in terms of integral data collection and demonstration the up-to-the-date predictive power of codes applied in designing hybrid (ADS) systems that use tungsten targets cooled with sodium [1, 2].

Foreword

The quantitative information describing interaction of accelerated proton with a target is necessary in designing even demo ADS. Application of hadron-nuclei process simulation should be tested by special experiments in which irradiation conditions, target material composition and location approximate the design type to the limit. There are several projects, [1] for example, where tungsten cooled by sodium is considered to be used as target material.

Tungsten belongs to the most promising materials for the multiplying targets of ADS facilities. Tungsten is sufficiently feasible technologically, shows the necessary set of nuclear-physics characteristics, and is devoid of any chemical reactivity and biological toxicity (as contrasted with, for example, lead and mercury). It should also be allowed for that the actual target designs involve not only the neutron generators made of heavy materials, but also the cooling and heat-exchanging units. Sodium is often regarded as a promising material for those units, considering that the sodium-based technologies have been studied in sufficient detail and mastered in designing and operating fast breeders.

This served as the basis for conducting experiment with a micromodel of a target containing tungsten and sodium. Comparison of experimental data obtained on such micromodel with corresponding calculated values will give us valuable information both for modification of codes and databases and for assessment of calculation accuracy of the target part of the relevant ADS facility designs.

Experiment plan

The target with alternating adherent tungsten and sodium discs was designed as such micromodel. The location of these discs which was specially chosen facilitates the maximum flattening of the neutron field along the target. Experimental samples made of ^{27}Al, ^{59}Co, ^{115}In, ^{197}Au, ^{209}Bi, ^{63}Cu, ^{65}Cu, ^{93}Nb, ^{64}Zn, ^{19}F (CF_2),

^{12}C, ^{181}Ta, ^{169}Tm which were manufactured by punching the corresponding foils or by molding fine powders and represent experimental samples 10.5 mm in diameter and 0.1–0.3 mm thick were placed inside the target and on its surface.

The layout of tungsten and sodium discs is shown in Fig. 1. All discs are 150 mm in diameter, disc thickness and sequence is listed in Table 1. The tungsten discs have special design providing insertion of special bars with round recesses for experimental samples to be placed inside the target. W (97.5%), Ni (1.75%), Fe (0.75%), and less than 0.2 % of impurities are incorporated in tungsten discs. The average density of the tungsten discs is 18.6 g/cm^3. Sodium discs represent metallic sodium placed into a steel container with 0.4 mm thick walls. Impurities content in Na is less than 0.02%. The discs are placed on a special adjustment table which provides alignment of target and proton beam axes with accuracy in the order of 1 mm.

The number of protons that hit the target, as well as the proton beam shape, were determined using an Al monitor placed along the beam at 5 cm in front of the first disc. After irradiation, the monitor was cut into separate fragments, most of which are 2×2cm squares. The number of ^{7}Be nuclei produced in each fragment was determined by γ-spectrometric analysis. Since the number of ^{7}Be nuclei produced in each of the fragments is proportional to the number of protons that traversed a fragment [1], the results make it possible to determine the number of protons that traversed each of the fragments, whereupon the proton beam shape can be restored. The monitor fragments are of large sizes (smaller sizes involve a great count error in the total absorption peak), so the beam shape was restored by least squares method on assumption the beam shape is described by the Gaussian along either of the x, y coordinates.

Target irradiation was performed with 0.8 GeV protons over a period of 10 hrs at the mean intensity $7.2{\cdot}10^{10}$ p/pulse using ITEP synchrotron. The pulse repetition rate is 15 pulses per minute. After short decay lag experimental samples were extracted from the target's surface and inside volume and packaged into labeled polyethylene packages. Subsequent gamma spectra measurements were taken using several spectrometers. The absolute values for different threshold reaction rates were determined using PCNUDAT decay database after gamma-spectra processing with GENIE2000 code.

[1] contrary to ^{7}Be, the ^{22}Na and ^{24}Na nuclei may be produced in the Al monitor due also to the neutrons emitted from the target backwards.

Simulation of reaction rates

The measured reaction rates were simulated using:

- the LAHET Code System[3] components, namely:

  1. the LAHET code to simulate high-energy hadron interactions with nuclei and transport in matter;
  2. the HMCNP code to simulate the transport of slow ($E_n < 20$) neutrons in matter.

  The LAHET code was set to allow for multiple scattering of primary protons and elastic scattering of neutrons above 20 MeV. The proton beam parameters were specified to conform to the results of determining the beam shape[2]. The hadron-nucleus interaction were simulated in terms of the ISABEL model. The neutron cross sections from the ENDF/B5 database were used in the HMCNP code.

- the KASKAD-S code system [4] which uses a discrete ordinate algorithm for coupled charges/neutral particle transport calculations in 2D pencil beam problems[3]. The multigroup cross-section library SADKO-2 for nucleon-meson cascade calculations coupled with CONSYST/ABBN-93 neutron and gammas cross-section libraries below 20MeV is used.

  The two code systems have yielded the neutron and proton energy spectra at the experimental sample locations.

- The package of nuclear databases with (p,x)- and (n,x)-cross sections of the measured reactions, including

  1. the MENDL2 [5] cross section database for the up-to 100 MeV neutron-induced reactions;
  2. the MENDL2P [6] cross section database for the up-to 200 MeV proton-induced reactions;

  In the cases where the high energy range ($100 < E < 800$MeV), which can contribute much to the measured reaction rates (Al, Co inside the target) is missing in the above databases, the cross sections from the databases were supplemented with the cross sections borrowed from experimental works.

[2] The beam is of σ_x=1.6cm, σ_y=1.0cm dimensions and is shifted 1.1 cm to the right.

[3] The beam was set as sum (superposition) of two beams centered at the target axis with σ_1=1.0cm and σ_2=1.6cm

Table 1: Disc sequence, thickness, and experimental samples layout.

Disc number	Material	Thickness, mm	Samples	
			Inside	Outside
W1	W	20	5Al*), Co	7Al, ^{115}In, Bi, Au, Ta
Na1	Na	3×40=120	-	-
W2	W	20	5Al, Co	Al, ^{115}In, Bi, Au, ^{169}Tm, ^{63}Cu, Ta, ^{65}Cu, ^{93}Nb, ^{64}Zn, ^{19}F, ^{12}C, Co
Na2	Na	2×40=80	-	-
W3	W	20	5Al, Co	7Al, ^{115}In, Bi, Au, Ta
Na3	Na	2×40=80	-	-
W4	W	20	5Al, Co	Al, ^{115}In, Bi, Au, Ta
Na4	Na	40	-	-
W5	W	40	5Al, Co	7Al, ^{115}In, Bi, Au, Ta
Na5	Na	40	-	-
W6	W	40	5Al, Co	Al, ^{115}In, Bi, Au, Ta
Na6	Na	40	-	-
W7	W	40	5Al, Co	7Al, ^{115}In, Bi, Au, Ta
Na7	Na	40	-	-
W8	W	40	5Al, Co	Al, ^{115}In, Bi, Au, Ta
Na8	Na	40	-	-
W9	W	40+20=60	5Al, Co	Al, ^{115}In, Bi, Au, Ta
Na9	Na	40	-	-
W10	W	2×40=80	5Al, Co	Al, ^{115}In, Bi, Au, Ta
Total		W: 380 Na: 520	50 Al, 10 Co	34 Al, 10 ^{115}In, 10 Bi, 10 Au, 10 Ta, ^{169}Tm, ^{63}u, ^{65}Cu, ^{93}Nb, ^{64}Zn, ^{19}F, ^{12}C, Co
		900	142 samples**)	

*) Al designates a single Al sample; 50 Al designates fifty Al samples, etc.
**) There are samples (made of Al) beside those specified in Table 1 for measuring the proton beam density distribution across the front (Al) surface and control of the neutron field uniformity along discs that form the target.

The simulated reaction rates were obtained by integral multiplying the spectra by the respective reaction cross sections

$$R = R_{n,x} + R_{p,x} = \sum_{i=n,p} \int \phi_i(E)\sigma_{i,x}(E)dE$$

.

The differences between the simulated and experimental reaction rates were estimated using the mean squared deviation factor $< F >$.

The experimental data together with the results of simulation using the LCS and KASKAD-S codes are presented in Figs. 2 and 3. Also presented is the mean squared deviation factor $< F >$.

Conclusions concerning the convergence of the calculated and experimental values

The LCS convergence

From Fig. 2 it follows that many of the reaction rates are predicted to a satisfactory accuracy (almost a half of the calculated values differ by less than 30% from the experimental data). At the same time, Fig. 2 demonstrate also some systematic deviation of the LCS calculations from experiment, namely,

1. the calculated data are much (up to factor 2) underestimated at the first three points of line C (target axis);

2. the calculated data are somewhat (up to factor 1.5) overestimated at the last point of line C;

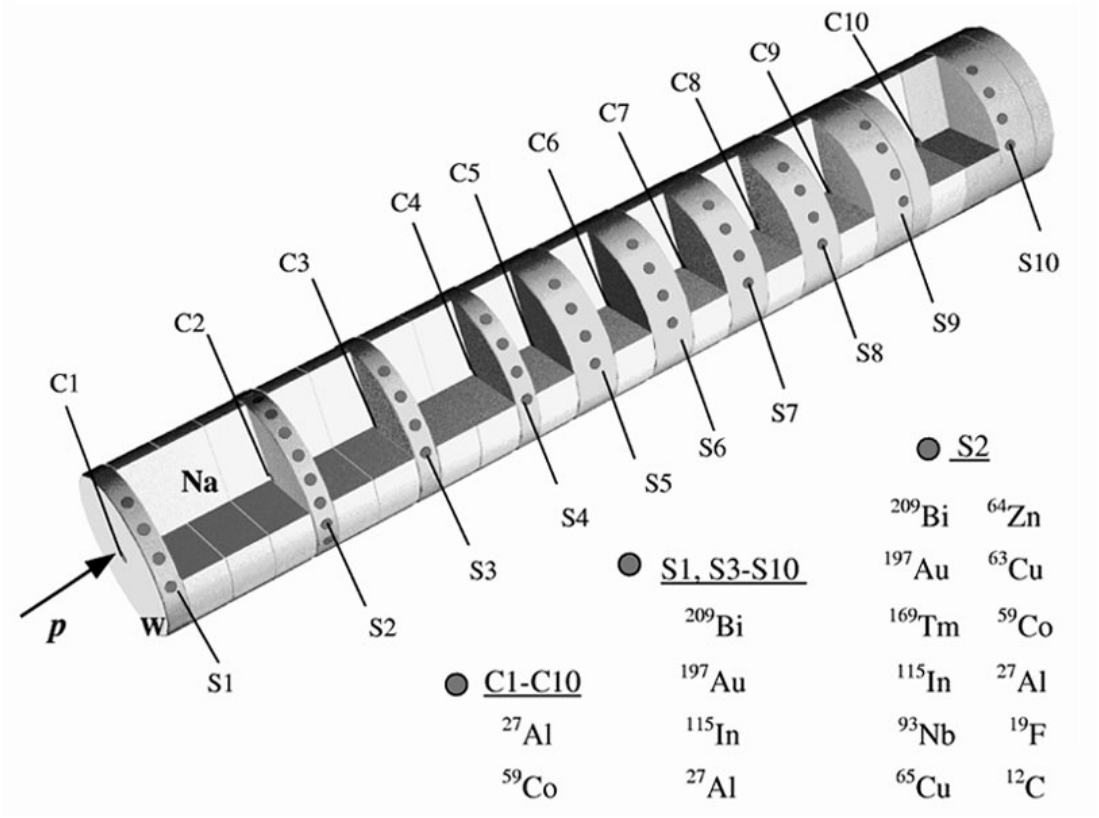

Figure 1: Layout of W and Na discs and experimental samples.

3. many of the calculated data tend to being overestimated at the first point of line S (target surface);

4. the ^{115}In(n,p)^{115}Cd reaction rate is much (up yo factor above 5) overestimated.

The systematic deviations can tentatively be explained as follows:

1. As seen from Fig. 2 for ^{59}Co$\rightarrow^{58}$Co and ^{27}Al$\rightarrow^{24}$Na reactions, protons contribute much to the reaction rates at the first points of line C. The the line S is located right on the proton beam axis, the beam geometry parameters affect much the proton fluxes at the points. Therefore, the actual significant deviation of the calculated reaction rates from experiment at the first points of line C, together with the minor deviations at the subsequent points of that line and at the points of line S, suggest that the Gaussian beam shape used in the calculations should be regarded as but an insufficiently adequate approximation.

2. The main contribution to the reaction rates at the last point is from the fast energy range neutrons whose energies exceed 20 MeV. The contribution from slow neutrons and secondary protons is underestimated because that poit is at the greatest distance from the target front surface. The deviation of calculations from experiment at that particular point may be accounted for a probable LAHET code inadequacy in the production and subsequent transport of the pre-equilibrium energy range neutrons.

3. At the first point of line S the main contribution to the reaction rates is from the neutrons and secondary protons produced in hadron-nucleus interactions with emission backwards and sidewards. A small underestimation of the reaction rates observed for some reactions at that particular point suggests that the LAHET code simulates rather inadequately the nuclean emission backwards.

4. The ^{115g}Cd ($T_{1/2}$=53.46h) production reaction rate has been determined experimentally, whereas the code simulation has given ^{115}Cd as a sum of all states (ground+isomeric). Therefore, the observed differences are not indicative of inadequate code simulation.

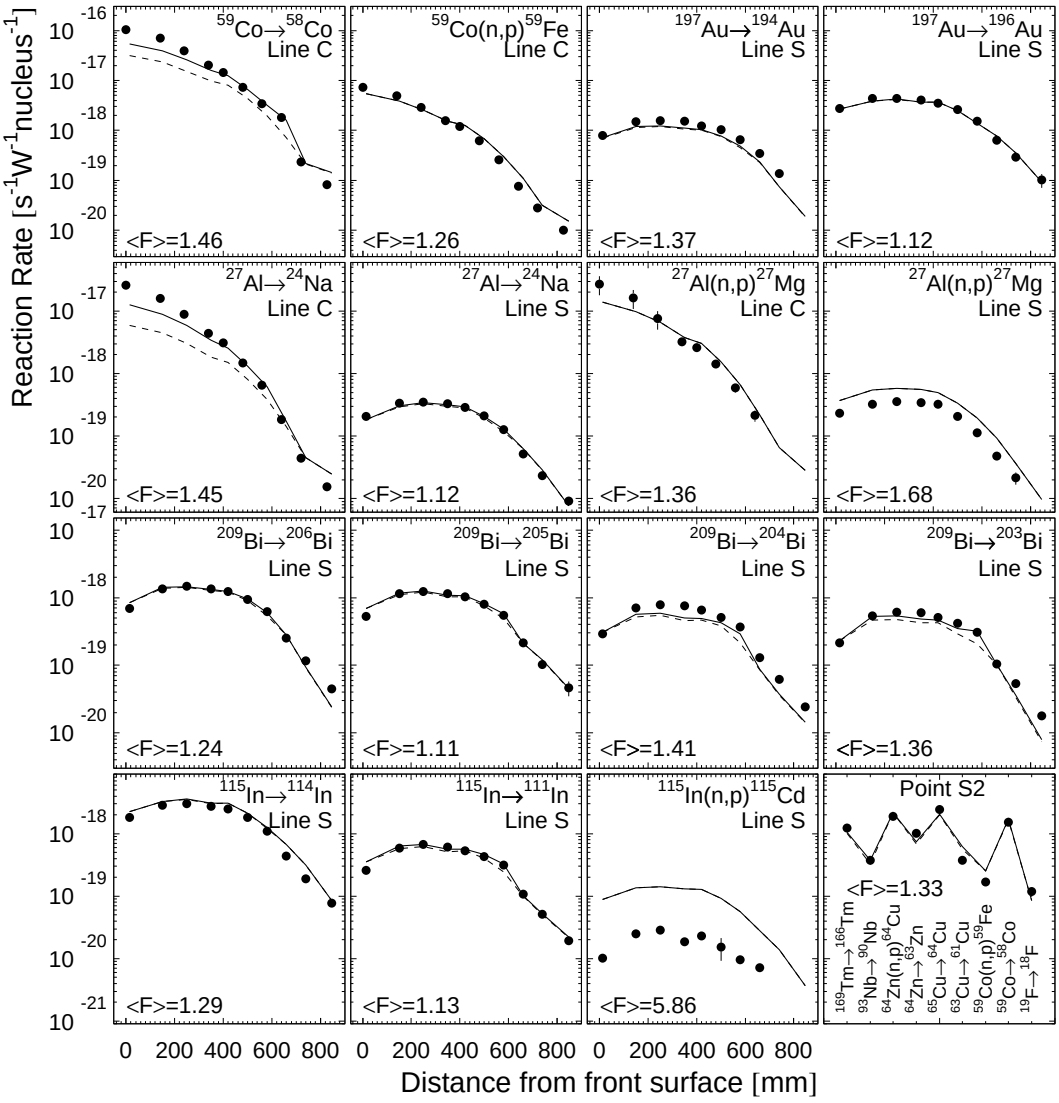

Figure 2: The experimental and the LCS calculated reaction rates. The dashed line is the neutron contribution. The mean squared deviation factor $< F >$ is also shown. The presented reaction rates have been normalized to the proton beam power.

It should be noted that the convergence of the experimental and simulated reaction rate data found here is better than the convergence of the like data on the cross sections for production of residual nuclides (see, for example, [7]). This fact is accounted for by the integral character of the reaction rates.

The KASKAD-S convergence

Fig. 3 shows the KASKAD-S–simulated reaction rates together with experimental data. The displayed results single out two data groups of a very different levels of agreement between the simulated and experimental results, namely, the target surface (line S) data and the target axis (line C) data.

Group (1) exhibits a comparatively good agreement of the simulated and experimental data (the rates of all reactions, other than ^{27}Al(n,p)^{27}Mg and ^{115}In(n,p)^{115}Cd, diverge from the experimental data by a factor of less than two). So, it is possible to conclude that, as a rule, the predictive power of the KASKAD-S code at the target points enough far from proton beam axis is about the same as the LAHET code predictive power.

Group (2) exhibits much worse agreement between the calculated and experimental results (all the simu-

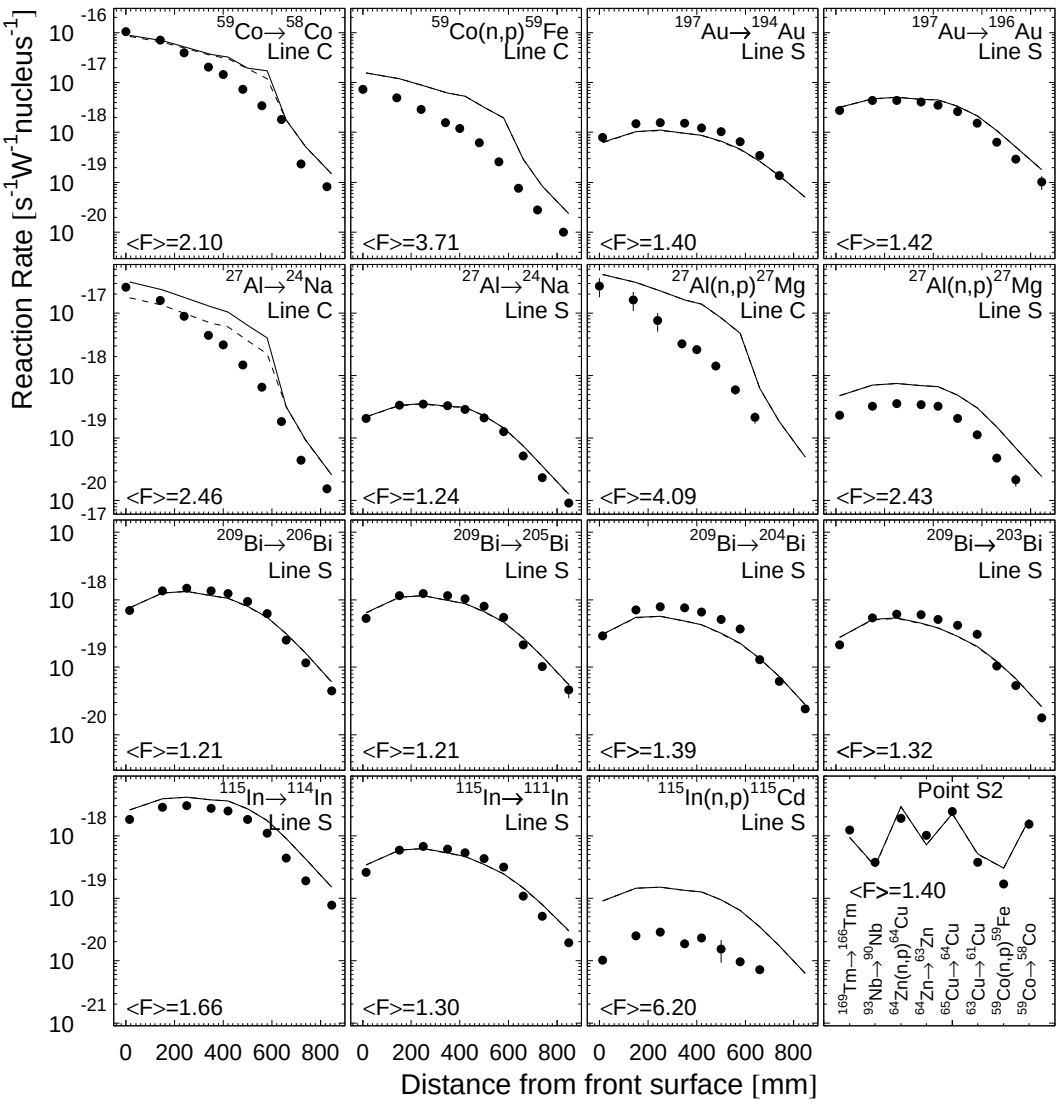

Figure 3: The experimental and the KASKAD-S calculated reaction rates. The dashed line is the neutron contribution. The mean squared deviation factor $< F >$ is also shown. The presented reaction rates have been normalized to the proton beam power.

lated reaction rates diverge from experiment by a factor of above two). An essential disagreement along line C can be explained similarly to the LAHET underestimation of reaction rates in the first points of line C, that is, by unadequate specifying of the beam geometry. The fact is that the KASKAD-S code simulates hadron cascade transport in 2D r, z geometry. That is why the axial symmetry of the proton beam is assumed in simulations. However, the real proton beam is not axially symmetric and the r, ϑ, z geometry calculation must be met to accurately simulate hadron transport in the vicinity of the target axis. A new 3D S_n code called KATRIN is under development with a view to resolving the problem.

Acknowledgement

The work has been carried out under the ISTC Project#1145 and supported by JAERI (Japan) and, partially, by the U. S. Department of Energy.

REFERENCES

[1] T. Takizuka et al, Conceptual Design Study of Accelerator-Driven Systems for Nuclear Waste

Transmutation, Proc. of the Second International Conference on Accelerator Driven Transmutation Technologies and Applications, June 3-7, 1996, Kalmar, Sweeden, pp. 179-185.

[2] G.J. Van Tuyle, D.E. Beller, Accelerator Transmutation of waste technology and implementation scenarios, Proc. of the Third Int. Topical meeting on Nuclear Applications of Accelerator Technology. Long Beach, CA, November 14-18, 1999, 337-346.

[3] R.E. Prael, H.Lichtenstein, LANL Report LA-UR-89-3014 (1989).

[4] M. Voloschenko, "An Algorithm for Spallation Target Neutronics and Shielding Calculations," Proc. of International Conference on Mathematics and Computations, Reactor Physics, and Environmental Analyses in Nuclear Applications, 27-30 September, 1999, Madrid, Spain, vol. 2, p. 975; A. M. Voloschenko, E. I. Yefimov, T. T. Ivanova,V. P. Kryuchkov and O. V. Sumaneev, "Using Discrete Ordinate Method in the SpallationTarget Neutronics and Shielding Calculations," Proc. 3-rd International Conference on Accelerator Driven Transmutation Technologies and Applications, June 7-11, 1999, Pruhonice, Chech Republic, Paper Code We-O-E12

[5] Yu.N. Shubin et al., Cross Section Data Library MENDL-2 to Study Activation and Transmutation of Materials Irradiated by Nucleons of Intermediate Energies, IAEA, INDC(CCP)-385, Vienna, May 1995.

[6] Yu.N. Shubin et al., Cross Section Data Library MENDL-2p to Study Activation and Transmutation of Materials Irradiated by Nucleons of Intermediate Energies, Nuclear Data for Science and Technology (Trietse 1997), IPS, Bologna, 1997, v.1., p.1054.

[7] Yu.E. Titarenko et al. "Exerimental and Theoretical Study ...., This proc.